

Upper critical field of $(\text{Bi,Pb})_2\text{Sr}_2\text{CaCu}_2\text{O}_8$ single crystals

Lu Zhang, J. Z. Liu, and R. N. Shelton

Department of Physics, University of California at Davis, Davis, California 95616

(Received 12 September 1991)

Reversible temperature-dependent magnetization measurements are conducted in fields up to 5 T on two $(\text{Bi,Pb})_2\text{Sr}_2\text{CaCu}_2\text{O}_8$ single crystals for fields along the c axis. A linear temperature dependence of the reversible magnetization has been obtained over a wide temperature range. The value of the magnetization slope dM/dT in the linear region at a fixed field decreases at higher field. Both the wide range of rounding of the magnetization near T_c and the field-dependent dM/dT in the $(\text{Bi,Pb})_2\text{Sr}_2\text{CaCu}_2\text{O}_8$ system indicate that the traditional extrapolation method based on a linear Abrikosov formula near H_{c2} may not be applied. A theoretical model is employed to determine the Ginzburg-Landau parameter κ and upper critical field H_{c2} versus temperature. For these two crystals, we find $\kappa=94$ and 89, and $H_{c2}(0)=95$ and 83 T, respectively, for fields parallel to the c axis.

I. INTRODUCTION

One crucial experimental property of high- T_c superconductors is their extraordinarily high upper critical field H_{c2} . Typical values of H_{c2} of high- T_c superconductors, such as 100 T for $\text{YBa}_2\text{Cu}_3\text{O}_{7-\delta}$ crystals below 1 K, are much larger than the strongest static magnetic fields achievable at present. Numerous applications of high- T_c superconductors in strong magnetic fields depend on this property.¹ Upper critical field studies in the high- T_c superconductors also give important information about the intrinsic properties of the mixed state for type-II superconductors. Due to experimental complexities of research at ultrahigh magnetic fields,² much work on H_{c2} has been done at low fields by analysis of resistivity and ac-susceptibility data using traditional methods for conventional superconductors. However, this approach is complicated in high- T_c superconductors by an unusual broadening of the transition in the magnetic field due to the strong influence of flux-flow and flux-creep phenomena. It was argued that the upper-critical-field value obtained by resistivity and ac susceptibility may only present the onset field of flux-line motion since the magnetization curve becomes irreversible at those points.³⁻⁵ On the other hand, it was believed that the upper critical field determined by a dc magnetization measurement might give an alternative approach to the true value. To determine the nucleation temperature, $T_c(H)$, an extrapolation of the linear portion of the magnetic curve in the superconducting state to the normal-state value was employed. The H_{c2} values of $\text{YBa}_2\text{Cu}_3\text{O}_{7-\delta}$ single crystals were reported from a dc magnetization measurement in earlier work.^{6,7} This linear extrapolation is based on the linear Abrikosov formula at high field near H_{c2} .⁸

$$-4\pi M = \frac{H_{c2}(T) - H}{(2\kappa^2 - 1)\beta_A}$$

($\beta_A = 1.16$), where $H_{c2}(T)$ maintains a linear temperature dependence near T_c . However, the slope of dM/dT at a

fixed field varies for different fields, in conflict with the expected field-independent slope of the Abrikosov formula. Recently, Hao *et al.*⁹ developed a variational model to calculate the total Ginzburg-Landau free energy, including the vortex core energy. An analytic expression for the reversible magnetization was obtained in the field range of $H_{c1} < H < H_{c2}$. Based on this model, they also revised the London model in the intermediate-field region of $H_{c1} \ll H \ll H_{c2}$,¹⁰ and a simple trivial expression for the linear dependence of M versus $\ln H$ was obtained. However, this linear dependence varied for different ranges of the applied field, and so the two parameters used to determine H_{c2} from the M versus $\ln H$ data depended on the reduced field $H/H_{c2}(0)$.¹⁰ The H_{c2} value of a $\text{YBa}_2\text{Cu}_3\text{O}_{7-\delta}$ crystal determined from the logarithmic field dependence of the magnetization was recently reported by Welp *et al.*¹¹ In this paper, we report the magnetization curves in the reversible region below T_c for two $(\text{Bi,Pb})_2\text{Sr}_2\text{CaCu}_2\text{O}_8$ single crystals for fields oriented parallel to the c axis. Values of κ and the upper critical fields $H_{c2}(T)$ are determined using the model of Hao *et al.*,⁹ thus yielding $H_{c2}(0)$, ξ_{ab} , and λ_{ab} .

II. EXPERIMENT

High-quality single crystals $(\text{BiPb})_2\text{Sr}_2\text{CaCu}_2\text{O}_8$ were prepared by a self-flux method.¹² To achieve quantitative and reproducible results, two crystals grown from different batches with sharp superconducting transitions were selected for the magnetization measurements. Each crystal had a mass of about 1 mg and dimensions of $1 \times 1 \times 0.1$ mm.³

Figure 1 shows the Meissner [field-cooled (FC)] and shielding [zero-field-cooled (ZFC)] curves for two single crystals of $(\text{BiPb})_2\text{Sr}_2\text{CaCu}_2\text{O}_8$. The applied field was 1 Oe parallel to the c axis. The experimental curves indicate a superconducting transition temperature at 94 K with a 10–90% transition width of about 2–3 K. The demagnetization factor D is about 0.9 for both crystals.

The magnetization experiments were performed on a

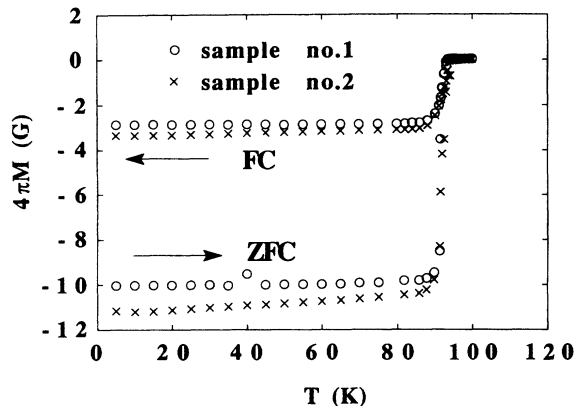


FIG. 1. Shielding (ZFC) and Meissner (FC) measurements in two $(\text{BiPb})_2\text{Sr}_2\text{CaCu}_2\text{O}_{8-\delta}$ crystals for $H=1$ Oe and $\mathbf{H}\parallel c$.

commercial superconducting quantum interference device (SQUID) magnetometer.¹³ The SQUID was operated with a scan length of 3 cm (Ref. 14) and an iterative regression mode was used to calculate the moment.

The reversible magnetization region reflects an equilibrium state and is not affected by flux motion. In order to measure the reversible magnetizations at various fields, we first measure the irreversible temperature T_r , which is defined as the low-temperature boundary of the reversible range. The measurement sequence consisted of cooling to a temperature well below T_r in zero field, applying a magnetic field, and warming up to above T_c (ZFC) and then cooling to the low temperature with the same field (FC). The increasing temperature steps for warming and cooling were 1 K. The irreversible temperatures $T_r(H)$ versus field is shown in Fig. 2, which is similar to the data of c axis-oriented powders of $\text{Bi}_2\text{Sr}_2\text{CaCu}_2\text{O}_8$.¹⁵ The inset of Fig. 2 shows a measurement result of a $(\text{BiPb})_2\text{Sr}_2\text{CaCu}_2\text{O}_8$ crystal in the temperature range 40–80 K at 0.1 T where T_r is determined as 52 K from an observable derivation between the FC and ZFC curves. The figure illustrates the large temperature region of reversible flux motion in the $(\text{BiPb})_2\text{Sr}_2\text{CaCu}_2\text{O}_8$ system. Above the irreversible temperature, the magneti-

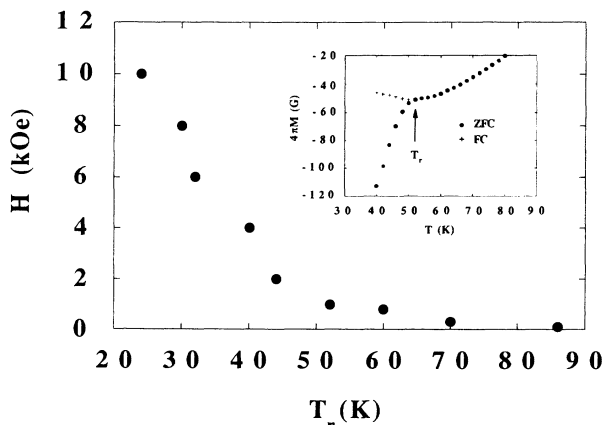


FIG. 2. Irreversible temperature measurement for field parallel to the c axis of a $(\text{BiPb})_2\text{Sr}_2\text{CaCu}_2\text{O}_{8-\delta}$ crystal.

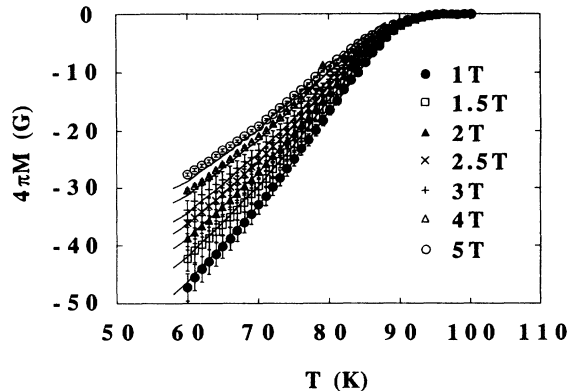


FIG. 3. Magnetization vs temperature for fields parallel to the c axis of a $(\text{BiPb})_2\text{Sr}_2\text{CaCu}_2\text{O}_{8-\delta}$ crystal. Solid lines indicate fit to theory.

zation displays a small amount of curvature, then takes on a nearly linear temperature dependence at still higher temperatures. The deviation of the linear magnetization at a temperature just above T_r may be due to a small amount of flux pinning.

The reversible magnetization was measured at fields up to 5 T and temperatures between 60 and 100 K. A normal-state baseline was observed to be temperature independent from T_c to 150 K, which indicates the background was due to the sample holder and could be subtracted from the data. Figure 3 exhibits the resultant magnetization in the reversible region at different fields oriented perpendicular to the ab plane. An error of $\pm 5\%$ was estimated from these measurements. In the reversible region, we observed that the magnetization showed a nearly linear temperature dependence (see Fig. 4) except for the curvature and rounding found near T_c . The slope $4\pi(dM/dT)$ varies from -68 G/K at 0.5 T to -87 G/K at 5 T. The range of this curvature extended to about 10 K below T_c for the $(\text{BiPb})_2\text{Sr}_2\text{CaCu}_2\text{O}_8$ crystals with the field parallel to the c axis.

III. RESULTS AND DISCUSSION

For an isotopic infinite type-II superconductor in the mixed state, Ginzburg-Landau theory expresses the free-

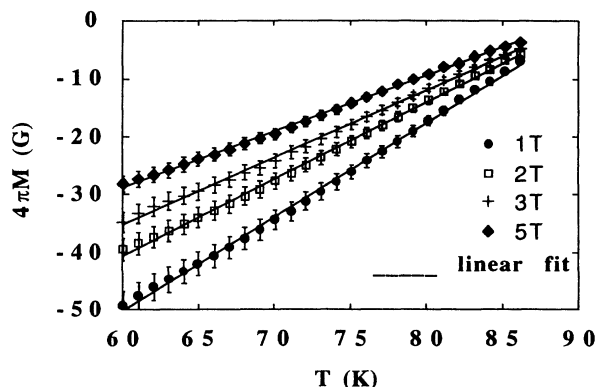


FIG. 4. Linear temperature dependence of magnetization for fields parallel to the c axis of a $(\text{BiPb})_2\text{Sr}_2\text{CaCu}_2\text{O}_{8-\delta}$ crystal.

energy density in dimensionless units as¹⁶

$$F_{SH} = F_{S0} + \frac{1}{2} - |\Psi|^2 + \frac{1}{2} |\Psi|^4 + \left| \left[\frac{1}{ik} \nabla - \mathbf{A} \right] \Psi \right|^2 + \mathbf{h}^2,$$

where F_{SH} and F_{S0} are the free-energy density of superconducting state in a magnetic field and zero magnetic field, respectively. Ψ is a complex order parameter, \mathbf{h} is the microscopic magnetic field, and \mathbf{A} is the vector potential corresponding to the local magnetic field.

The Ginzburg-Landau equations have the form

$$\left[\frac{1}{iK} \nabla - \mathbf{A} \right]^2 \Psi = \Psi (1 - |\Psi|^2),$$

$$\mathbf{j} = \nabla \times \mathbf{h} = \frac{1}{2} \left[\Psi^* \left[\frac{1}{ik} \nabla - \mathbf{A} \right] \Psi - \Psi \left[-\frac{1}{ik} \nabla - \mathbf{A} \right] \Psi^* \right].$$

Hao *et al.*⁹ introduced two variational parameters ξ_v and f_∞ representing the effective core radius of a vortex and the depression in the order parameter due to the overlapping of vortices, and assumed the order parameter to have the form

$$\Psi = \Psi_0 f e^{-i\phi},$$

where

$$f = \frac{\rho}{\sqrt{\rho^2 + \xi_v^2}} f_\infty.$$

Ψ_0 is the magnitude of order parameter in absence of field and ρ, ϕ are the cylindrical coordinates for a vortex centered on the z axis.

The thermodynamic magnetic field H was given by

$$H = -4\pi M + B = \frac{1}{2} \frac{dF}{dB} = H(B, f_\infty, \xi_v, \kappa) \quad (1)$$

and the two variational parameters satisfied

$$\frac{\partial F}{\partial f_\infty} = 0, \quad (2)$$

$$\frac{\partial F}{\partial \xi_v} = 0, \quad (3)$$

where the detailed expressions of Eqs. (1)–(3) are given in the Appendix. These nonlinear equations include three variables B, f_∞, ξ_v for a given H and κ . In the theoretical model, the authors used approximated solutions of Eqs. (2) and (3) [see Eqs. (24) and (25) in Ref. 9] and solved Eq. (1) numerically. Here, we employed an iteration method for solving Eqs. (1)–(3) simultaneously. In the analysis, we considered the difference of the values between dimensionless units and conventional units. We chose a set of data $\{4\pi M, H\}$ at the fixed temperature in the reversible region, where $4\pi M$ is the magnetization and H is the applied field. Assuming a value of κ , B' (the prime denotes dimensionless units) can be obtained from the ratio of $4\pi M / (H - D4\pi M) = 4\pi M' / H'$ by solving the above equations simultaneously, where D is the demagnetization factor and $H - D4\pi M$ is the corresponding effective field. Because the magnitude of the

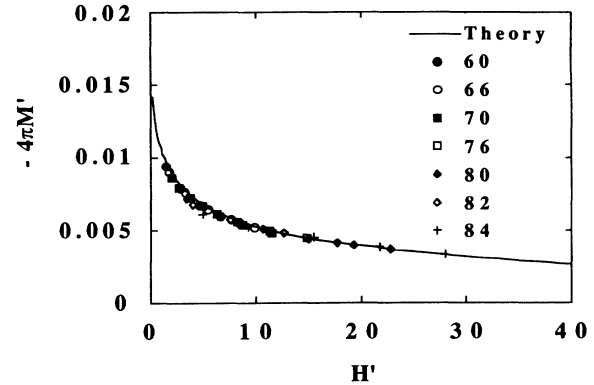


FIG. 5. Magnetization vs field in dimensionless units for a $(\text{BiPb})_2\text{Sr}_2\text{CaCu}_2\text{O}_{8-\delta}$ crystal at $\mathbf{H}||c$ where the solid line corresponds to the theoretical fitting.

magnetization is much smaller than the applied field, the demagnetization effect is very small. The magnetization $4\pi M'$ and applied field H' can be calculated from B' : $4\pi M' / H' = B' / H' - 1$. Therefore,

$$\sqrt{2}H_c(T) = \frac{H - D4\pi M}{H'} = \frac{4\pi M}{4\pi M'}$$

can be found for various fields for a given κ . The value of κ is determined to have the smallest deviation of the value $\sqrt{2}H_c(T)$ from all the data of the different fields by the assumption of κ being temperature independent. The $H_{c2}(T) = \kappa \sqrt{2}H_c(T)$ is then calculated. The data points used in the theoretical fitting to obtain κ and $H_c(T)$ are from the reversible linear magnetization in the range $60 < T < 85$ K and $0.5 < H < 5$ T. The best fits to the experimental data give $\kappa = 94 \pm 4$ for sample no. 1 and $\kappa = 92 \pm 5$ for sample no. 2. The ranges of error are about $\pm 5\%$ which came from the fitting. The large values of κ suggest that the $(\text{BiPb})_2\text{Sr}_2\text{CaCu}_2\text{O}_8$ system is an extreme type-II superconductor.

Figures 3 and 5 show $4\pi M$ versus T and $4\pi M'$ versus H' of the experimental measurements with corresponding theoretical fittings as indicated by solid lines in conventional units and dimensionless units, respectively. Both figures display the excellent fit to the model. The magnetization $4\pi M'$ in Fig. 6 also shows a logarithmic depen-

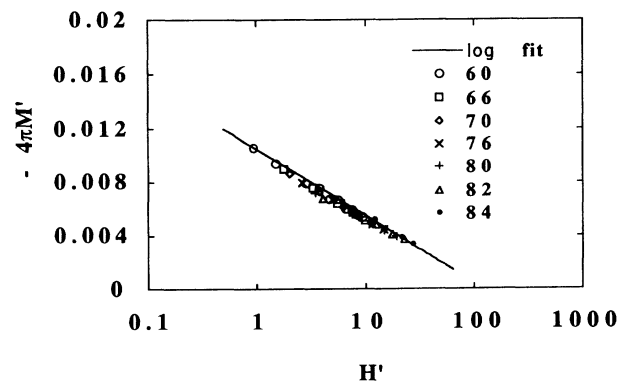


FIG. 6. Logarithmic dependence of magnetization in dimensionless units for a $(\text{BiPb})_2\text{Sr}_2\text{CaCu}_2\text{O}_{8-\delta}$ crystal at $\mathbf{H}||c$.

dence on H' which is qualitatively consistent with the prediction of London model in the intermediate-field region:

$$-4\pi M' = \frac{1}{4\kappa} \ln \left[\frac{\eta\kappa}{H'} \right],$$

where η is a constant of order unity. Since the London model neglected the important effect of depression of the order parameter to zero at the vortex center, Hao and Clem suggested a modification:¹⁰

$$-4\pi M' = \frac{\alpha}{4\kappa} \ln \left[\frac{\beta\kappa}{H'} \right], \quad (4)$$

where $\alpha=0.84$ and $\beta=1.23$ are found by fitting in the field range of $1 < H' < 50$ (or $0.01 < H/H_{c2} < 0.5$).

The critical fields $H_{c2}(T)$ are shown in Fig. 7 which give the slope of $dH_{c2}(T)/dT$ near T_c as -1.5 and -1.3 T/K for samples 1 and 2, respectively. The orbital critical fields extrapolated to $T=0$ K using the Werthamer-Helfand-Hohenberg (WHH) formula¹⁷

$$H_{c2}(0) = 0.69 \left| \frac{dH_{c2}(T)}{dT} \right|_{T_c} T_c$$

are $H_{c2}(0)=95$ and 83 T for two samples at fields parallel to the c axis. These values are comparable to those obtained from microwave measurements¹⁸ and are larger than those determined from resistivity measurements.¹⁹ $H_{c2}(T)$ is about 26 T at 77 K and rising to above 90 T at low temperature, which is much larger than conventional commercial superconductors. For Nb-Ti, T_c is 9 K and $H_{c2}(4 \text{ K}) = 11$ T, and for Nb₃Sn it is 22 T with $T_c = 18$ K. Therefore, the high- T_c superconductors are not only conceptually interesting in attempts to understand the microscopic magnetism, but also of practical interest because of potential strong-magnetic-field applications.

To find the coherence length at zero temperature, we use the expression $H_{c2}(0)_{\parallel} = \phi_0 / 2\pi \xi_{ab}^2(0)$, where $\phi_0 = 2.07 \times 10^{-7}$ G cm² is the flux quantum. $\xi_{ab}(0) = 1.9$ and 2.0 nm are then calculated assuming the clean limit. The short coherent length, several orders smaller than in conventional superconductors, gives rise to only a few Cooper pairs within one coherence volume and leads to pronounced fluctuation effects at the transition into superconducting state. In the fit of the data, the large and temperature dependent κ was found in the temperature range about 10 K below T_c , which is unexpected from Ginzburg-Landau mean-field theory where κ is expected

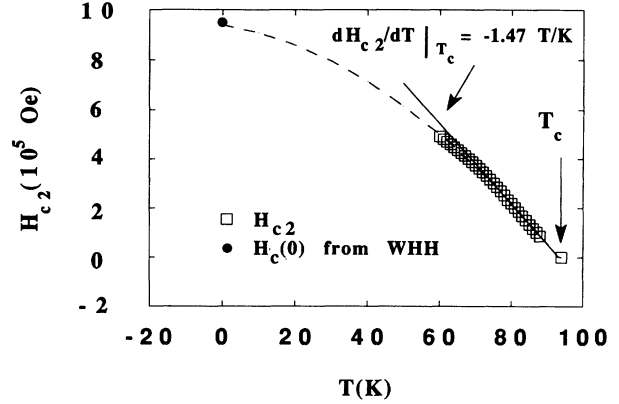


FIG. 7. Upper critical field vs applied field at $H_{\parallel}c$ of a (BiPb)₂Sr₂CaCu₂O_{8- δ} crystal.

as constant near T_c . This region also shows the curvature and rounding curves as we mentioned before. This behavior might be explained due to diamagnetic fluctuations or minor sample inhomogeneities.

London penetration depth λ_{ab} 's are estimated as 178 nm for both crystals, in good agreement with the result of 172 nm, from direct penetration depth measurement obtained from a muon spin rotation experiment.²⁰

IV. CONCLUSION

In conclusion, we have used the reversible, linear temperature dependence of the dc magnetization of (BiPb)₂Sr₂CaCu₂O₈ crystals to determine the equilibrium upper critical fields of this material. Compared with YBa₂Cu₃O_{7- δ} , (BiPb)₂Sr₂CaCu₂O₈ crystals have a large reversible magnetization region and smaller flux pinning.¹² Thus, the theory based on an equilibrium state without pinning is more applicable to this oxide system. The critical field slope dH_{c2}/dT of (BiPb)₂Sr₂CaCu₂O₈ crystals is found to be -1.4 ± 0.1 T/K for the c direction averaged over the two samples. A fluctuation region was observed at high temperatures $T > 0.9T_c$. Using the WHH formalism, the zero-temperature orbital critical fields are 89 ± 6 T, and the associated coherent lengths and London penetration depths are $\xi_{ab}(0) = 2.0 \pm 0.1$ nm $\lambda_{ab}(0) = 178 \pm 8$ nm, respectively.

ACKNOWLEDGMENTS

This research was supported by the U.S. Department of Energy under contract No. W-7405-ENG-48 to Lawrence Livermore National Laboratory and by the National Science Foundation under Grant No. DMR-90-21029.

APPENDIX

The complete form of Eqs. (1)–(3) presented in the Results and Discussion section is given below. Parameters are identified in the text with the exception of K_0 and K_1 , which are modified Bessel functions of the zeroth and first orders, respectively:

$$H = \frac{\kappa f_\infty^2 \xi_v^2}{2} \left[\frac{1-f_\infty^2}{2} \ln \left[\frac{2}{B\kappa\xi_v^2} + 1 \right] - \frac{1-f_\infty^2}{2+B\kappa\xi_v^2} + \frac{f_\infty^2}{(2+B\kappa\xi_v^2)^2} \right] + \frac{f_\infty^2 (2+3B\kappa\xi_v^2)}{2\kappa(2+B\kappa\xi_v^2)^3} \\ + B + \frac{f_\infty}{2\kappa\xi_v K_1(f_\infty \xi_v)} \left[K_0(\xi_v(f_\infty^2 + 2B\kappa)^{1/2}) - \frac{B\kappa\xi_v K_1(\xi_v(f_\infty^2 + 2B\kappa)^{1/2})}{(f_\infty^2 + 2B\kappa)^{1/2}} \right], \quad (\text{A1})$$

$$\frac{\partial F}{\partial f_\infty} = 0 = -2f_\infty(1-f_\infty^2) + B\kappa\xi_v^2 f_\infty \left[(1-2f_\infty^2) \ln \left[\frac{2}{B\kappa\xi_v^2} + 1 \right] + \frac{2f_\infty^2}{2+B\kappa\xi_v^2} \right] + \frac{2Bf_\infty(1+B\kappa\xi_v^2)}{\kappa(2+B\kappa\xi_v^2)^2} \\ + \frac{B}{\kappa\xi_v K_1(f_\infty \xi_v)} \left[2K_0(\xi_v(f_\infty^2 + 2B\kappa)^{1/2}) - \frac{\xi_v f_\infty^2 K_1(\xi_v(f_\infty^2 + 2B\kappa)^{1/2})}{(f_\infty^2 + 2B\kappa)^{1/2}} \right. \\ \left. + \frac{f_\infty \xi_v K_0(f_\infty \xi_v) K_0(\xi_v(f_\infty^2 + 2B\kappa)^{1/2})}{K_1^2(f_\infty \xi_v)} \right], \quad (\text{A2})$$

$$\frac{\partial F}{\partial \xi_v} = 0 = B\kappa\xi_v f_\infty^2 \left[(1-f_\infty^2) \ln \left[\frac{2}{B\kappa\xi_v} + 1 \right] - \frac{2(1-f_\infty^2)}{2+B\kappa\xi_v^2} + \frac{2f_\infty^2}{(2+B\kappa\xi_v^2)^2} \right] - \frac{2\kappa B^3 f_\infty^2 \xi_v^3}{(2+B\kappa\xi_v^2)^3} \\ - \frac{Bf_\infty^2}{\kappa\xi_v K_1(f_\infty \xi_v)} \left[\frac{(f_\infty^2 + 2B\kappa)^{1/2} K_1(\xi_v(f_\infty^2 + 2B\kappa)^{1/2})}{f_\infty} - \frac{K_0(f_\infty \xi_v) K_0(\xi_v(f_\infty^2 + 2B\kappa)^{1/2})}{K_1(f_\infty \xi_v)} \right]. \quad (\text{A3})$$

¹David Larbalestier, Phys. Today **44**, 74 (1991).

²Y. Tajima, M. Hikita, T. Ishii, H. Fuke, K. Sugiyama, M. Date, A. Yamagishi, A. Katsui, Y. Hidaka, T. Iwata, and S. Tsurumi, Phys. Rev. B **37**, 7956 (1988).

³Y. Yeshurun and A. P. Malozemoff, Phys. Rev. Lett. **60**, 2202 (1988).

⁴A. P. Malozemoff, T. K. Worthington, Y. Yeshurun, F. Holtzberg, and P. H. Kes, Phys. Rev. B **38**, 7203 (1988).

⁵C. Rossel, Y. Maeno, and I. Morgenstern, Phys. Rev. Lett. **62**, 681 (1989).

⁶U. Welp, W. K. Kwok, G. W. Crabtree, K. G. Vandervoort, and J. Z. Liu, Phys. Rev. Lett. **62**, 1908 (1989).

⁷K. G. Vandervoort, U. Welp, K. Kessler, H. Claus, G. W. Crabtree, W. K. Kwok, and J. Z. Liu, Phys. Rev. B **43**, 13042 (1991).

⁸A. A. Abrikosov, Zh. Eksp. Teor. Fiz. **32**, 1442 (1957).

⁹Zhidong Hao, John R. Clem, M. W. McElfresh, L. Civale, A. P. Malozemoff, and F. Holtzberg, Phys. Rev. B **43**, 2844 (1991).

¹⁰Zhidong Hao and John R. Clem, Phys. Rev. Lett. **67**, 2371 (1991).

¹¹U. Welp, S. Fleshler, W. K. Kwok, K. G. Vandervoort, J. Downey, B. Veal, and G. W. Crabtree (unpublished).

¹²Lu Zhang, J. Z. Liu, M. D. Lan, P. Klavins, and R. N. Shelton, Phys. Rev. B **44**, 10190 (1991).

¹³Quantum Design, Inc., San Diego, CA.

¹⁴Quantum Design, Inc., MPMS Tech. Note, 1989 (unpublished).

¹⁵Y. Xu, M. Suenaga, Y. Gao, J. E. Crow, and N. D. Spencer, Phys. Rev. B **42**, 8756 (1990).

¹⁶A. L. Fetter and D. C. Hohenberg, in *Superconductivity*, edited by R. D. Parks (Marcel Dekker, New York, 1969), Vol. II, p. 817.

¹⁷N. R. Werthamer, E. Helfand, and P. C. Hohenberg, Phys. Rev. **147**, 295 (1966).

¹⁸H. A. Blackstead, D. B. Pulling, P. J. McGinn, and J. Z. Liu, Physica C **174**, 394 (1991).

¹⁹M. J. Naughton, R. C. Yu, P. K. Davis, J. E. Fischer, R. V. Chamberlin, Z. Z. Wang, T. W. Jing, N. P. Ong, and P. M. Chaikin, Phys. Rev. B **38**, 9280 (1988).

²⁰M. Weber, P. Birrer, F. N. Gyax, B. Hitti, E. Lippelt, H. Maletta, and A. Scheneck, Hyperfine Interact. **63**, 93 (1990).